Journal of Constructional Steel Research xxx (2017) xxx–xxx

Contents lists available at ScienceDirect

Journal of Constructional Steel Research

Review

Performance of concrete filled stainless steel tubular (CFSST) columns and joints: Summary of recent research

Lin-Hai Han [a,*], Chuan-Yang Xu [a], Zhong Tao [b]

[a] Department of Civil Engineering, Tsinghua University, Beijing 100084, China
[b] Centre for Infrastructure Engineering, Western Sydney University, Penrith, NSW 2751, Australia

ARTICLE INFO

Article history:
Received 10 January 2018
Accepted 27 February 2018
Available online xxxx

Keywords:
Concrete filled stainless steel tubes
Material properties
Bond strength
Static performance
Dynamic performance
Fire performance
Design approach

ABSTRACT

Concrete filled stainless steel tubular (CFSST) columns have attracted increasing research interests in the last decade. This paper briefly introduces the material properties of stainless steel and reviews recent research on behaviour of CFSST columns and joints at both ambient and elevated temperatures. The reviewed studies include tests of bond behaviour between the stainless steel tube and core concrete, and the static behaviour of CFSST stub columns, slender columns, beams, stainless steel-concrete-carbon steel double-skin tubular columns, and concrete filled bimetallic tubular columns. The cyclic behaviour of CFSST beam-columns under combined axial and lateral cyclic loading as well as the impact behaviour of CFSST columns is also introduced. Fire test results of full-scale CFSST columns are presented along with finite element analysis results. The behaviour of composite joints with CFSST columns is also briefly reviewed in this paper. Based on the previous research, future research directions on CFSST are summarised and discussed.

Contents

1. Introduction

In the last few decades, the application of stainless steel in construction has attracted increasing interests among researchers and structural engineers. Compared with conventional carbon steel, stainless steel has several advantages, such as extremely high durability and corrosion resistance, easiness of maintenance and improved fire resistance. However, the high cost of stainless steel prevents its wide application as a structural material. To make more economical use of stainless steel, it is advisable to develop stainless steel-concrete composite structures. A good example is to fill stainless steel hollow sections with concrete to

* Corresponding author.
E-mail address: lhhan@tsinghua.edu.cn (L.-H. Han).

https://doi.org/10.1016/j.jcsr.2018.02.038
0143-974X/

form concrete filled stainless steel tubes (CFSST). Fig. 1 shows typical cross-sections of circular and square CFSST columns, where D is the diameter of the circular steel tube, and B is the width of the square steel tube.

In the past, extensive studies have been conducted on conventional concrete filled carbon steel columns and their behaviour has been well understood. Since the material behaviour of stainless steel is different from that of conventional carbon steel, some recent studies have been carried out to investigate the behaviour of CFSST members and joints. This is necessary to allow the development of any rational design guidelines for this type of innovative composite structure.

This paper reviews the state-of-the-art of concrete filled stainless steel tubular members and joints at ambient or elevated temperatures. Experimental investigations on the bond behaviour of CFSST [1–3], members and joints under various loading conditions, including static loading [4–17], dynamic loading [18–22] and fire [23,24], as well as joints under static loading [25–27] and fire [28], are summarised in Table 1. The following key points are presented in the paper to have a better understanding of CFSST members and joints:

(1) Mechanical properties of stainless steel under different service conditions are summarised to fully understand the behaviour of stainless steel tubes. The differences of mechanical properties between carbon steel and stainless steel are discussed.
(2) Bond behaviour of CFSST columns is discussed and several methods have been recommended to enhance the bond strength in particular regions.
(3) Failure modes and load versus deformation curves of CFSST columns with various cross-section types under different loading conditions are stated in comparison with conventional concrete filled steel tubular (CFST) columns manufactured with carbon steel.
(4) Cyclic tests on CFSST columns show that the columns have high strength and ductility and good energy-dissipation capacity, justifying the use in seismic-prone areas. Meanwhile, impact tests on CFSST columns demonstrate that they can be used as piers in bridges or as exterior columns in buildings.
(5) Behaviour of CFSST columns in fire and after fire exposure is worth discussing due to the superior performance of stainless steel at elevated temperatures.
(6) Composite joints, including hybrid beam-column joints, T-joints and X-joints, are commonly used in engineering practice. The behaviour of composite joints with CFSST members is also briefly introduced.

2. Stainless steel material and tubes

2.1. Stainless steel grades

Stainless steels are alloys of iron containing at least 10.5% chromium and usually at least 50% iron [29]. Variations in chemical composition and heat treatment generate different grades of stainless steels for engineers to choose. Three categories of stainless steels are recommended in Eurocode 3 [30] for structural applications, including ferritic, austenitic and duplex (austenitic-ferritic) alloys. Ferritic stainless steels generally have the lowest price and worst corrosion resistance among the three categories, which can be attributed to the rare content of nickel in the composition. Meanwhile, ferritic stainless steels are less weldable than other stainless steels due to embrittlement of the heat-affected zones. However, they generally have better engineering properties than austenitic grades. Austenitic stainless steels, as the most commonly used stainless steel, provide a good combination of corrosion resistance, weldability, forming and fabrication properties [31]. Duplex stainless steels have a mixed microstructure of austenite and ferrite. Compared with austenitic stainless steels, duplex stainless steels have higher strengths, similar weldability, lower formability and similar or higher corrosion resistance.

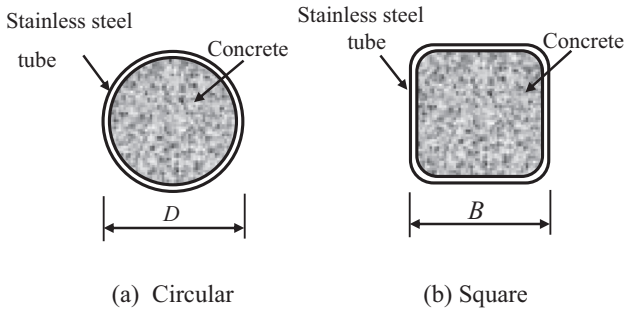

Fig. 1. Typical cross-sections of concrete filled stainless steel tubes.

Table 2 summarises grades of several frequently used structural stainless steels in EN 10088-1 [32], ASTM A959 [33] and GB/T 20878 [34] along with the major chemical compositions according to EN 10088-1 [32]. The nominal yield stress (f_y) and ultimate strength (f_u) of each stainless steel grade specified in EN 10088-2 [35] are shown in Table 3. To select the most appropriate grade of stainless steel, the environment of the application, the fabrication route, the surface finish and the maintenance of the structure should be considered.

2.2. Stress–strain behaviour at room temperature

Stainless steels demonstrate different stress–strain (σ - ε) behaviour when compared with carbon steels. Fig. 2 shows typical stress–strain curves for both stainless steel and carbon steel [36]. In general, carbon steel demonstrates linear elastic behaviour up to the yield stress, and there is often a plateau before strain hardening is encountered. In contrast, stainless steel has a more rounded response without a well-defined yield stress. For this reason, the 0.2% proof stress is usually used to define the nominal yield stress (f_y). Stainless steel usually has excellent ductility. The elongation after fracture for austenitic stainless steels can often reach 60–70% under tension, whilst that for duplex stainless steels can reach 40–50%.

To describe the nonlinear σ- ε curves of stainless steel, Rasmussen [37] proposed a full-range σ - ε relationship expressed by Eq. (1):

$$\varepsilon = \begin{cases} \dfrac{\sigma}{E} + 0.002\left(\dfrac{\sigma}{f_y}\right)^n & \text{for } \sigma \le f_y \\ 0.002 + \dfrac{f_y}{E} + \dfrac{\sigma - f_y}{E_y} + \varepsilon_u\left(\dfrac{\sigma - f_y}{f_u - f_y}\right)^m & \text{for } f_y < \sigma \le f_u \end{cases} \quad (1)$$

where E and E_y are the initial elastic modulus and the tangent modulus of the stress–strain curve at the yield stress, respectively; f_u and ε_u are the ultimate strength and the corresponding strain, respectively; and m and n are parameters.

Eq. (1) has been recommended in the Eurocode 3 [30]. In this equation, n is used to describe the degree of nonlinearity of the stress–strain curve. A lower value of n implies a greater degree of nonlinearity. When n is infinity, a perfectly elastic-plastic material model is obtained.

It should be noted that, equations have been proposed by Rasmussen [37] to predict f_u and ε_u of stainless steel based on regression analysis of test data. However, the predictions are generally more accurate for austenitic and duplex stainless steels than for ferritic stainless steels. This is due to the fact that only 12 test data of ferritic alloys were available when Rasmussen's model was developed. The accuracy of Rasmussen's model was recently evaluated by Arrayago et al. [38], where more than 1000 measured σ - ε curves of austenitic, ferritic and duplex stainless steel coupons were used in the comparison. The prediction accuracy of Rasmussen's model for austenitic and duplex alloys was confirmed, whilst a revised model was proposed for ferritic alloys to improve the prediction accuracy. Similarly, Tao and Rasmussen [39]

Please cite this article as: L.-H. Han, et al., Performance of concrete filled stainless steel tubular (CFSST) columns and joints: Summary of recent research, J Constr Steel Res (2017), https://doi.org/10.1016/j.jcsr.2018.02.038

Table 1
Summary of experiment researches on CFSST members and joints.

Loading type	Test type	No.	Grade of stainless steel tube	f_y (MPa)	Concrete type	f_c' (MPa)	Number of specimens	Section type	Reference
Bond behaviour	Push-out tests	1	Austenitic–EN 1.4301	321–521	NC/RAC/EC	40.4–81.8	12	Circular and square	Tao et al. [1]
		2	–	420	NC	25.8[a]–41.4[a]	32	Circular	Chen et al. [2]
		3	Austenitic–EN 1.4301	336–378	NC/EC	40.4–57.5	40	Circular and square	Song et al. [3]
Static loading	Stub columns under axial loading	4	Austenitic–EN 1.4301	259–440	NC	20.0–34.9	54	Circular and square	Uy et al. [4]
		5	–	266–458	NC	30–74	12	Circular and square	Lam et al. [5]
		6	Duplex–EN 1.4462 High strength austenitic	448–536	NC	46.6–83.5	14	Square and rectangular	Young et al. [6]
		7	Austenitic–EN 1.4301	286.7	RAC/NC	44.24[a]–50.72[a]	14	Circular and square	Yang and Ma [7]
		8	Austenitic–EN 1.4301	301.5–339.6	RAC/NC	37.8–41.7	8	Circular and rectangular	Tam et al. [8]
		9	Austenitic–EN 1.4401	270.3–324.4	SSC	31.4	6	Circular and double skin	Li et al. [9]
		10	Austenitic–EN 1.4401	225.7–281.1	SSC	35.8–39.4	6	Circular and double skin	Li et al. [10]
		11	–	319.6	SCC	52.5[a]	54	Stainless steel-concrete-carbon steel double skin	Han et al. [11]
		12	Austenitic–EN 1.4301	300	NC	40.5–115.6	14	Stainless steel-concrete-carbon steel double skin	Wang et al. [12]
		13	Austenitic–EN 1.4541	274.6–283.3	NC	16.9[a]–34.2[a]	10	Bimetallic circular	Ye et al. [13]
		14	Austenitic–EN 1.4301	285	NC	27.8[a]–49.5[a]	10	Stiffened square and rectangular	Dabaon et al. [14]
	Slender columns under axial loading	15	Austenitic–EN 1.4301	288.6–390.3	NC	36.3–75.4	24	Circular, square and rectangular	Uy et al. [4]
		16	Austenitic–EN1.4547	324	FRC/NC	31.2[a]–33.6[a]	3	Circular	Ellobody et al. [15]
	Columns under eccentric loading	17	Austenitic–EN 1.4301	358–435	NC	12	6	Circular and square	Uy et al. [4]
		18	Austenitic–EN1.4547	324	FRC/NC	31.2[a]–33.6[a]	8	Circular	Ellobody et al. [15]
		19	–	650	SFRC/NC	40.14–60.51	15	Square	Tokgoz et al. [16]
	Beams under pure bending	20	Austenitic	423–471	NC	32[a]–40.8[a]	16	Square and rectangular	Chen et al. [17]
		21	Austenitic–EN 1.4301	286.7	RAC/SCC	44.24[a]–50.72[a]	14	Circular and square	Yang and Ma [7]
Dynamic loading	Columns under cyclic lateral loading	22	Austenitic–EN 1.4301	362.1–385.1	RAC/NC	51.9[a]–52.3[a]	10	Circular and square	Liao et al. [18]
	Beam-columns under cyclic loading	23	Austenitic–EN 1.4301	264.4–379.1	NC	42.7[a]–62.6[a]	24	Stainless steel-concrete-stainless steel double skin	Zhou et al. [19]
	Columns under impact lateral loading	24	Austenitic–EN 1.4301	382–587	NC	91.6	3	Square	Bambach et al. [20]
		25	Austenitic–EN 1.4301	610	NC	41	1	Square	Yousuf et al. [21]
		26	Austenitic–EN 1.4301	444	NC	16	2	Square	Yousuf et al. [22]
Fire	Columns in fire	27	Austenitic–EN 1.4301	346–451	SCC	51.4[a]	5	Circular and square	Han et al. [23]
		28	Austenitic–EN 1.4301	292.9–307.9	NC	41.4–46.6	12	Circular and square	Tao et al. [24]
Joints	Composite joints	29	Austenitic–EN 1.4301	339–367	NC	32.8–42.3	6	Beam-column joints	Tao et al. [25]
		30	Austenitic–EN 1.4301 Duplex–EN 1.4462 High strength austenitic	320–707	NC	27.5–29.5	11	T-joints	Feng and Young [26]
		31	Austenitic–EN 1.4301 Duplex–EN 1.4462 High strength austenitic	447–707	NC	24.9–29.1	25	X-joints	Feng and Young [27]
		32	–	292.3–315.1	NC	39.5[a]–46.6[a]	7	Beam-column joints	Song et al. [28]

Note:
1. NC means normal concrete; RAC means recycled aggregate concrete; EC means expansive concrete; SCC means self-consolidating concrete; FRC means fibre reinforced concrete; SFRC means steel fibre reinforced concrete.
2. The strength of concrete cubes ($150 \times 150 \times 150$ mm in size) denoted with superscript (a) has been multiplied by a coefficient of 0.8 to be recorded as concrete cylinder strength f_c' in the table.

Table 2
Grades and chemical compositions of several frequently used stainless steels.

Type	Grade			Major chemical composition according to EN 10088			
	EN 10088-1:2005	ASTM A959-2009	GB/T 20878-2007	C	Cr	Ni	Mo
Austenitic	1.4301	304	06Cr19Ni10	0.07	17.5–19.5	8.0–10.5	–
	1.4401	316	06Cr17Ni12Mo2	0.07	16.5–18.5	10.0–13.0	2.0–2.5
	1.4541	321	06Cr18Ni10Ti	0.08	17.0–19.0	9.0–12.0	–
Duplex	1.4162	S32101	–	0.04	21.0–22.0	1.35–1.9	0.1–0.8
	1.4462	S32205/S31803	–	0.03	21.0–23.0	4.5–6.5	2.5–3.5
Ferritic	1.4003	S40977	022Cr12	0.03	10.5–12.5	0.3–1.0	–
	1.4521	444	019Cr19Mo2NbTi	0.025	17.0–20.0	–	1.8–2.5

conducted further research to collect a total of 56 tensile test data of ferritic stainless steel coupons. Accordingly, new equations were proposed to predict f_u and ε_u of ferritic stainless steel. Thus, the accuracy of the revised σ- ε model has been greatly improved in predicting σ - ε curves of ferritic alloys.

Anisotropic behaviour, particularly at low strains, is often observed for stainless steels. This means that the mechanical behaviour in longitudinal direction may be different from that in transverse direction. Meanwhile, stainless steels also display non-symmetry of tensile and compressive behaviour. Anisotropy and non-symmetry is more significant for cold-worked steel. In general, austenitic steels show less material anisotropy and non-symmetry and this effect may be ignored [40]. But it is more pronounced for duplex and ferritic steels. Based on the interpretation of experimental data, Quach et al. [40] proposed a three-stage stress–stain model for stainless steels using the three basic Ramberg-Osgood parameters (E, f_y and n), where the influence of non-symmetry was incorporated in the model. Meanwhile, the mechanical properties specified in the Australian and American codes [31,41] for different stainless steel grades take account of the anisotropy and non-symmetry, which are not considered in Eurocode 3 [30].

2.3. Strength enhancement induced during cold forming

Currently, stainless steel square or rectangular hollow sections are mainly formed by cold rolling. Similar to carbon steel, there is significant strength enhancement at the corner regions of cold-formed sections, and this effect in stainless steel is even more pronounced than in carbon steel. The strength enhancement of stainless steel at the corner regions is commonly between 20% and 100% in terms of 0.2% proof strength compared with the flat regions [42]. However, a decrease in the ultimate strain $\varepsilon_{u,c}$ is observed for the corner material of cold-formed hollow sections [43]. Austenitic stainless steels demonstrate significant strength enhancement at corner regions of cold-formed sections, which is attributed to the combined effects of the deformation-induced dislocations and martensitic-phase transformation. In contrast, the deformation hardening is less significant for duplex and ferritic stainless steels because of the lack of martensite transformation in the alloys [39].

Table 3
Nominal yield stress and ultimate strength of several frequently used stainless steels in EN 10088.

Type	Grade (EN)	Cold rolled strip: $t \le 8$ mm		Hot rolled strip: $t \le 13.5$ mm		Hot rolled plate: $t \le 75$ mm	
		f_y (MPa)	f_u (MPa)	f_y (MPa)	f_u (MPa)	f_y (MPa)	f_u (MPa)
Austenitic	1.4301	230	540	210	520	210	520
	1.4401	240	530	220	530	220	520
	1.4541	220	520	200	520	200	500
Duplex	1.4162	530[a]	700[a]	480[b]	680[b]	450	650
	1.4462	500	700	460	700	460	640
Ferritic	1.4003	280	450	280	450	250[c]	450[c]
	1.4521	300	420	280	400	280[d]	420[d]

[a] $t \le 6.4$ mm.
[b] $t \le 10$ mm.
[c] $t \le 25$ mm.
[d] $t \le 12$ mm.

Therefore, to accurately analyse the nonlinear behaviour of CFSST members, several models have been developed for different grades of corner stainless steels.

Based on the analysis of test data, Cruise and Gardner [44] proposed a model expressed by Eq. (2) to predict the enhanced corner material strength.

$$f_{y,c} = \frac{1.673 f_y}{(r_i/t)^{0.126}} \tag{2}$$

where $f_{y,c}$ and f_y are the 0.2% proof stresses of the corner material and the virgin material, respectively; r_i is the internal corner radius; and t is the thickness of the cross-section.

The properties of the virgin material, however, are often not available for commercial hollow structural sections. In this case, the increased yield stress of the corner material may be predicted using the ultimate strength (f_u) of the flat faces as follows [44]:

$$f_{y,c} = 0.83 f_u \tag{3}$$

Stress–strain models are required to conduct an accurate structural analysis. A revised Rasmussen's model was proposed by Wang et al. [43] to predict σ–ε curves for corner regions of square/rectangular austenitic and duplex stainless steel tubes. This model expressed by Eq. (4) was proposed based on a total of 85 tests results and 24 full-range σ–ε curves.

$$\varepsilon = \begin{cases} \dfrac{\sigma}{E} + 0.002\left(\dfrac{\sigma}{f_{y,c}}\right)^{n_c} & \text{for } \sigma \le f_{y,c} \\ 0.002 + \dfrac{f_{y,c}}{E} + \dfrac{\sigma - f_{y,c}}{E_{y,c}} + \varepsilon_{u,c}\left(\dfrac{\sigma - f_{y,c}}{f_{u,c} - f_{y,c}}\right)^{m_c} & \text{for } f_{y,c} < \sigma \le f_{u,c} \end{cases} \tag{4}$$

where E is the initial elastic modulus of the flat material; $E_{y,c}$ expressed by Eq. (5) is the tangent modulus of the stress–strain curve of the corner material at the yield stress; $f_{y,c}$ and $f_{u,c}$ expressed by Eqs. (6) and (7) are the yield stress and ultimate strength of the corner material, respectively; $\varepsilon_{u,c}$ expressed by Eq. (8) is the ultimate strain corresponding to $f_{u,c}$ of the corner material; and m_c and n_c expressed by Eqs. (9) and (10) respectively are parameters for the corner material.

$$E_{y,c} = \frac{E}{1 + 0.002\ n_c E / f_{y,c}} \tag{5}$$

$$\frac{f_{y,c}}{f_y} = 1 + 0.05\left(\frac{f_y}{E}\right)^{900/f_y} \tag{6}$$

$$\frac{f_{u,c}}{f_{y,c}} = \left(0.56 f_y^{0.226} - 1.4\right)\frac{f_u}{f_y} \tag{7}$$

$$\varepsilon_{u,c} = 1 - \frac{f_{y,c}}{f_{u,c}} \tag{8}$$

$$m_c = 0.04 f_y - 8 \ge m \tag{9}$$

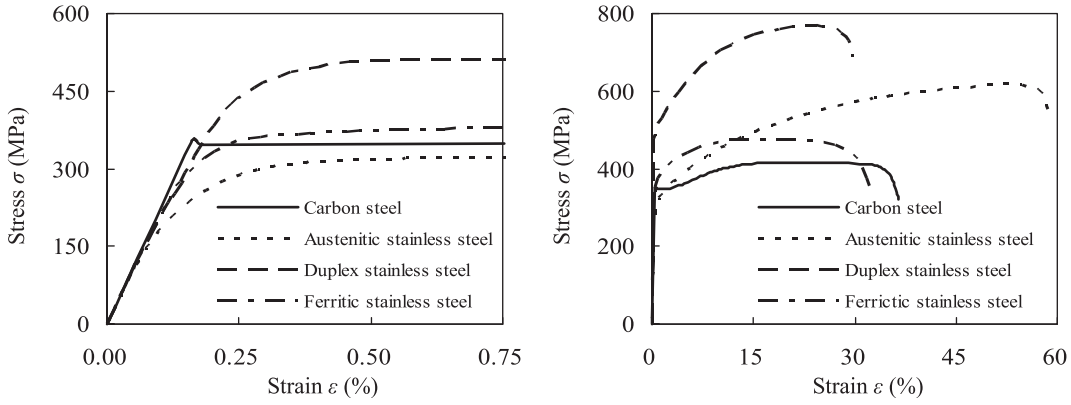

(a) Initial stage of σ–ε curves (b) Full range σ–ε curve

Fig. 2. Typical stress–strain curves for stainless steel and carbon steel.

$$n_c = 0.9n^2\left(\frac{f_y}{E}\right)^{-0.3n} \tag{10}$$

Further research was conducted by Tao and Rasmussen [39] to propose a σ–ε model for corner regions of square/rectangular ferritic stainless steel tubes. Eq. (4) was still used for ferritic stainless steel, but the corresponding $f_{y,c}$ and $f_{u,c}$ were expressed by Eqs. (11) and (12), respectively.

$$\frac{f_{y,c}}{f_y} = 0.25 + \frac{E}{500f_y} \geq 1 \tag{11}$$

$$\frac{f_{u,c}}{f_{y,c}} = \left(1.55 - \frac{E}{840f_y}\right)\frac{f_u}{f_y} \tag{12}$$

It should be noted that f_u in Eq. (12) should be determined by Eq. (13) proposed specifically for ferritic stainless steel in [39].

$$\frac{f_y}{f_u} = \begin{cases} 0.104 + 360\dfrac{f_y}{E} & \text{for } 0.00125 \leq f_y/E \leq 0.00235 \\ 0.95 & \text{for } 0.00235 < f_y/E \leq 0.00275 \end{cases} \tag{13}$$

The σ–ε models proposed in [39,43] can capture the mechanical properties of corner materials of different types of stainless steel very well. The accuracy of these models has been validated by comparing with the test results. The use of these models would increase the simulation accuracy of cold-formed stainless steel structures.

2.4. Residual stresses

Membrane stresses and bending residual stresses can be detected in a cold-formed stainless steel member, resulting from the plastic deformation occurred during the coiling and uncoiling of the sheet material and forming of the section. In general, the effects of bending residual stresses are inherently present in a stress–strain model, and only membrane stresses induced through welding need to be considered. Previous investigations by Ashraf et al. [45] and Gardner and Nethercot [46] have shown that the residual stresses cause only a small reduction in initial stiffness but have little influence on the overall load–deformation response for a stainless steel column. A similar conclusion has been reached in the investigation by Ellobody and Young [47], where measured residual stresses were used in the finite element (FE) modelling. The influence of bending and membrane residual stresses on global and local buckling of stainless steel square hollow tubes was further investigated by Jandera et al. [48]. Interestingly, it was found that the inclusion of residual stresses even led to a slight increase in load-carrying capacity.

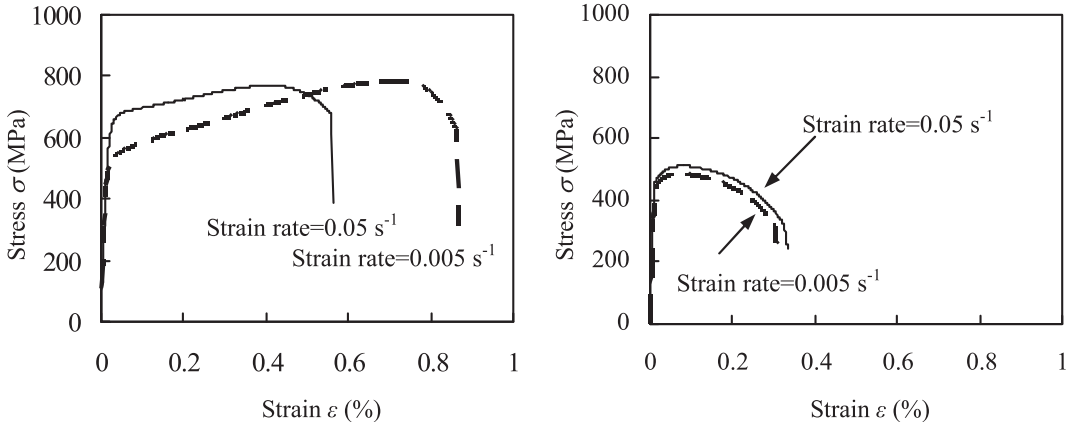

(a) Stainless steel (EN 1.4301) (b) Carbon steel

Fig. 3. Effect of strain rate on the stress-strain curves of stainless and carbon steels.

Please cite this article as: L.-H. Han, et al., Performance of concrete filled stainless steel tubular (CFSST) columns and joints: Summary of recent research, J Constr Steel Res (2017), https://doi.org/10.1016/j.jcsr.2018.02.038

It is expected that the influence of residual stresses will be further minimised for a concrete filled steel tubular (CFST) column by concrete filling. This beneficial influence of concrete in-fill has been demonstrated in previous investigations [49]. Hence, the residual stresses may be ignored in modelling CFSST columns.

2.5. Effect of strain rate

Stainless steels have a stronger strain rate dependency than carbon steel, especially in the region of 0.2% proof strain [29]. Quasi-static tests were conducted by Uy et al. [50] on both stainless and carbon steel coupons using a MTS material testing machine under strain rates of 0.005 s^{-1} and 0.05 s^{-1}, respectively. The measured σ- ε curves for the stainless steel (austenitic grade 1.4301) and carbon steel materials are shown in Fig. 3a and b, respectively. For the carbon steel, the yield stress increased by 4.5% when the strain rate increased from 0.005 s^{-1} to 0.05 s^{-1}, whilst that for the stainless steel increased by 24.7% under the same condition. In contrast, the ultimate strength for the carbon steel increased from 487 MPa to 512 MPa when the strain rate increased from 0.005 s^{-1} to 0.05 s^{-1}; whilst the ultimate strength for stainless steel decreased slightly from 785 MPa to 771 MPa. As can be seen, distinct strain rate effect is observed for both the stainless steel and carbon steel materials. However, much higher strain rate sensitivity is found for the stainless steel material as shown in Fig. 3a. Although the stainless steel showed much higher ductility than the carbon steel, the elongation of the stainless steel under the strain rate of 0.05 s^{-1} decreased significantly compared with that under the stain rate of 0.005 s^{-1}. No such phenomenon was observed for the carbon steel material, as shown in Fig. 3b.

Due to the significant strain rate sensitivity and high ductility of stainless steels, a high strain rate enhancement factor can be used in design to take advantage of the increase in strength at higher strain rates [29]. For this reason, stainless steels are suitable to be used in blast walls, crash barriers or other structural members susceptible to blast and/or impact loading.

2.6. Thermal properties and stress–strain behaviour in fire

Due to the variation in chemical composition, thermal properties of stainless steel also differ from those of carbon steel. Ferritic and duplex steels have a thermal expansion similar to carbon steel. But austenitic stainless steel has a higher thermal expansion than carbon steel. At room temperature, the coefficient of thermal expansion for the former is approximately 17×10^{-6}/°C compared to 12×10^{-6}/°C for carbon steel [51].

Before reaching a temperature of 800 °C, thermal conductivity of stainless steel is lower than that of carbon steel [51]. At room temperature, stainless steel has a thermal conductivity of about 15 W/m K compared to about 53 W/m K for carbon steel. The lower thermal conductivity tends to lead to higher thermal gradients in stainless steel. On average, the specific heat of stainless steel is slightly lower than that of carbon steel. The specific heat of stainless steel is approximately 550 J/kg K as compared with approximately 600 J/kg K for carbon steel [52]. Furthermore, stainless steel has a lower emissivity than carbon steel. In Eurocode 3 [51], 0.4 and 0.7 are specified for stainless steel and carbon steel, respectively.

At elevated temperatures, stainless steel offers better retention of strength and stiffness than carbon steel. According to the models given in Eurocode 3 [51], stress–strain curves of stainless steel and carbon steel at 600 °C are compared in Fig. 4. Obviously, stainless steel retains much higher strength at a comparatively large deformation due to the effect of strain-hardening and good ductility. In general, it is believed that stainless steel structures have better fire performance than carbon steel structures. However, the higher thermal expansion of austenitic stainless steel and higher thermal gradients in stainless steel might have some detrimental influence, which should be considered in structural fire design.

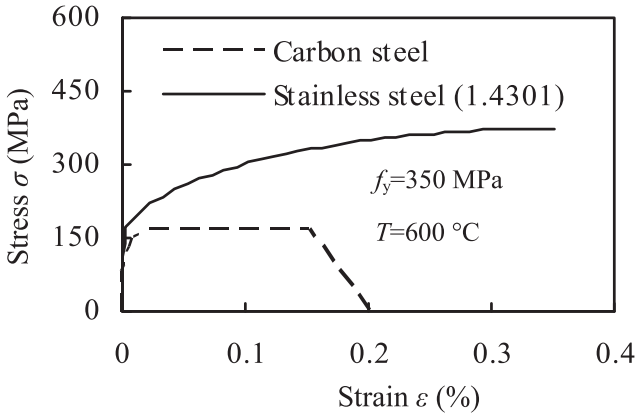

Fig. 4. Stress-strain curves of stainless steel and carbon steel at 600 °C.

2.7. Post-fire stress–strain curves

Fire safety has always been an important issue for structures. If a structure does not collapse during a fire, the priority will be to assess whether it can be reused or not. To fulfil this task, post-fire models of materials will be required. With the increasing use of stainless steel in structures, there is a need to investigate the stress–strain curves of stainless steel after fire exposure.

Wang et al. [43] carried out tensile tests to evaluate the post-fire behaviour of austenitic stainless steels, where flat and corner coupons cut from a square hollow section and curved coupons extracted from a circular hollow section were exposed to various temperatures (200–1000 °C) and heat soak times (0–135 min). The experimental results showed that compared with carbon steel, stainless steel has superior post-fire performance and higher strength retention capacity, as shown in Fig. 5. Furthermore, fire exposure has a more obvious influence on the corner material than on the flat material. For flat and curved coupons, the yield stress demonstrates an obvious decrease only when the temperature T exceeds 500 °C. Similar phenomenon was reported by Ng and Gardner [53] for stainless steel tested in fire. For corner material, the strength enhancement due to cold forming starts to diminish with increasing T and a recovery in ductility can be observed.

Based on the test data, a post-fire stress–strain model was proposed to capture the mechanical properties of flat and corner austenitic

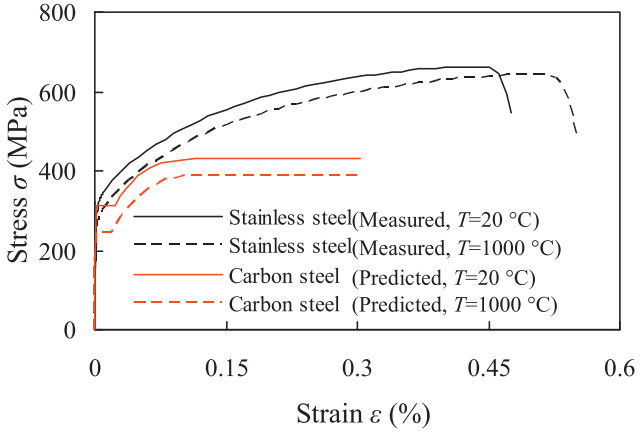

Fig. 5. Comparisons of stainless steel and carbon steel after exposure to fire.

Please cite this article as: L.-H. Han, et al., Performance of concrete filled stainless steel tubular (CFSST) columns and joints: Summary of recent research, J Constr Steel Res (2017), https://doi.org/10.1016/j.jcsr.2018.02.038

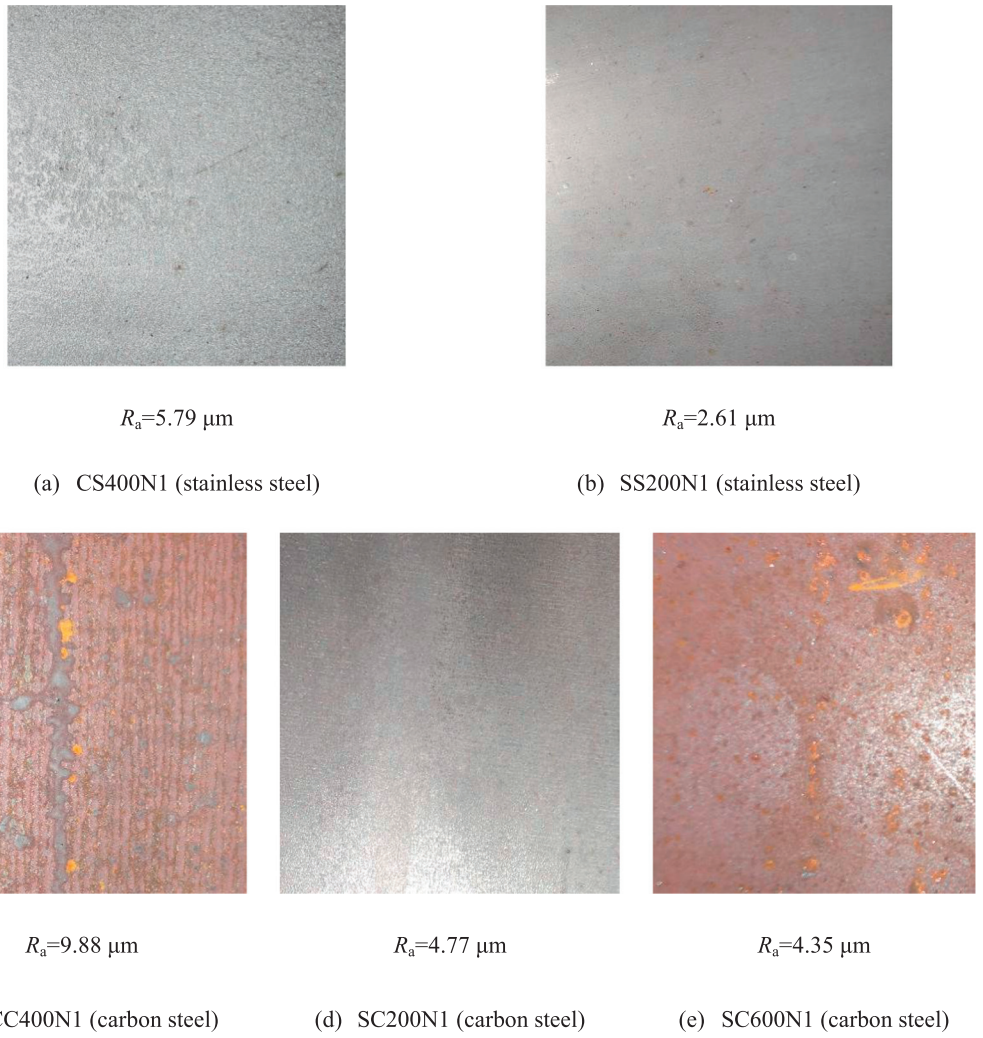

Fig. 6. Internal surface conditions of typical steel tubes.

stainless steels after exposure to elevated temperatures [43]. The model for flat austenitic stainless steels is expressed by Eq. (14).

$$\varepsilon = \begin{cases} \dfrac{\sigma}{E} + 0.002\left(\dfrac{\sigma}{f_{yT}}\right)^{n} & \text{for } \sigma \le f_{y,T} \\ 0.002 + \dfrac{f_{yT}}{E} + \dfrac{\sigma - f_{yT}}{E_{yT}} + \varepsilon_u\left(\dfrac{\sigma - f_{yT}}{f_u - f_{yT}}\right)^{m_T} & \text{for } f_{y,T} < \sigma \le f_u \end{cases} \tag{14}$$

where

$$E_{yT} = \frac{E}{1 + 0.002\ nE/f_{yT}} \tag{15}$$

$$m_T = 1 + 3.5\frac{f_{yT}}{f_u} \tag{16}$$

$$f_{yT} = \begin{cases} f_y & \text{for } T \le 500\ ^{\circ}\text{C} \\ \left[1 - 1.75 \times 10^{-4}(T-500) - 2.71 \times 10^{-7}(T-500)^2\right] f_y & \text{for } T > 500\ ^{\circ}\text{C} \end{cases} \tag{17}$$

It should be noted that a post-fire stress–strain model for corner regions has also been proposed in [43]. The model is expressed by an equation similar to Eq. (4).

More recently, an experiment investigation on duplex and ferritic stainless steels was conducted by Tao et al. [54] to investigate the post-fire performance. It is found that the ductility of austenitic and duplex alloys increases slightly after heated beyond 800 °C whilst the ductility of ferritic stainless steel reduces significantly after heated beyond 800 °C. Moreover, there is a reduction in yield stress and an increase in fracture strain for austenitic and duplex stainless steels. In general, austenitic alloy has the best performance after fire exposure, followed by mild steel and duplex alloy. Ferritic alloy has higher strength retention than high-strength steel, but the brittle failure of ferritic alloy after heated to 800 °C should be noticed. Based on the test results in [43,54], refined σ- ε models including a necking stage were proposed in [54] to describe the behaviour of austenitic, duplex and ferritic stainless steels after fire exposure.

3. Bond behaviour of concrete filled stainless steel tubes

Bond between the steel tube and core concrete could play a key role in the composite action between the two components. Sufficient bond strength is necessary to ensure the possible shear force transfer in a composite column. However, compared with the inner surface of a carbon steel tube, that of the stainless steel tube is generally smoother since it can be free of rust. This may lead to a reduction in the bond strength in stainless steel composite columns. In order to evaluate the influence of using stainless steel on the bond strength, Tao et al. [1] carried out push-out tests, where the main parameters were the cross-

Please cite this article as: L.-H. Han, et al., Performance of concrete filled stainless steel tubular (CFSST) columns and joints: Summary of recent research, J Constr Steel Res (2017), https://doi.org/10.1016/j.jcsr.2018.02.038

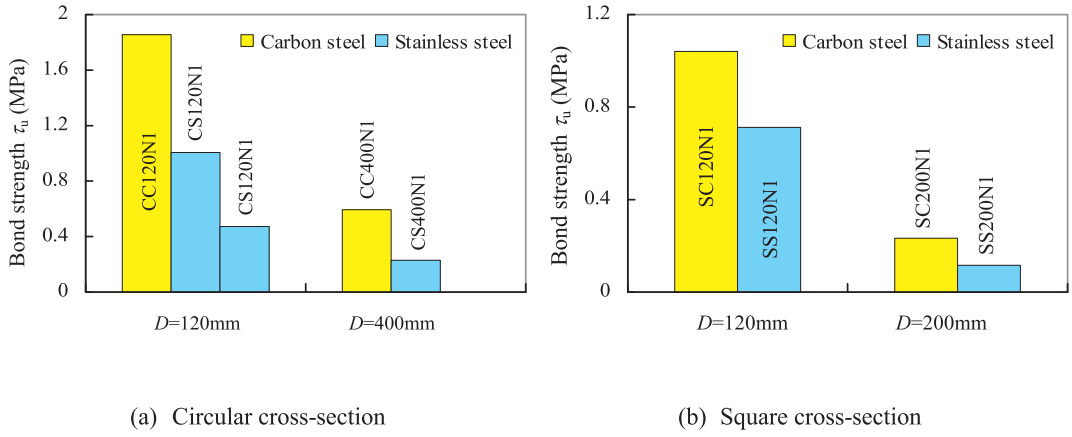

(a) Circular cross-section (b) Square cross-section

Fig. 7. Comparisons of bond strength between CFSST and CFST columns.

sectional dimension (120–600 mm), steel type (carbon and stainless steels), concrete type (normal, recycled aggregate and expansive concretes), concrete age (31–1176 days), and interface type (normal interface, interface with shear studs and interface with an internal ring). Before filling concrete, values of the average surface roughness (R_a) were measured for typical steel tubes. The typical surface conditions of stainless steel and carbon steel tubes are shown in Fig. 6 [1]. It was found that average surface roughness (R_a) of stainless steel could vary significantly among different products. The internal surface finish of the stainless steel tube in specimen SS200N1 represents typical 2B surface finish, whilst the internal surfaces of the tubes in specimens SC200N1 and SC600N1 are typical carbon steel surfaces with no or light rust. It was found that the R_a-value of a stainless steel tube was only about a half of that of the carbon steel counterpart. For this reason, the measured bond strengths between the stainless steel tube and concrete in CFSST columns decreased by 32% to 69% compared with the bond strengths in conventional CFST columns, as shown in Fig. 7.

For some regions in structures, the demands for bond may be very strong, such as connections, foundation supports, and braced frames. Therefore, the bond strength reduction in CFSST columns may need to be considered when there is a need of potential load transfer between the stainless steel tube and concrete. To enhance the bond strength, several approaches have been proposed in [1], such as welding internal ring (s) onto the inner surface of the steel tube, welding shear studs and using expansive concrete. Welding internal rings is the most effective method, followed by welding shear studs and adopting expansive concrete. However, further research is required to develop design guidelines to facilitate the use of these methods. Chen et al. [2] conducted a series of repeated push-out tests on CFSST columns. It was confirmed that about 70% of the bond strength in a CFSST column is from the interface friction force, whilst the remaining 30% of the bond strength is contributed by the chemical adhesive force and the mechanical interlock force.

Song et al. [3] carried out further tests to investigate the post-fire bond behaviour of CFSST columns, where the specimens were heated in the furnace to a target temperature of 800 °C before conducting the push-out test. They found that the bond strength of CFSST specimens was generally lower than that of the CFST specimens after fire. However, when the concrete age was relatively long (over six months), the influence of steel type on the bond strength was reduced due to the influence of concrete shrinkage.

4. Static performance

An experimental study on 117 specimens was carried out by Uy et al. [4], including 60 short CFSST columns under axial compression or combined actions of compression and bending, 24 CFSST slender columns and 33 reference short empty stainless steel hollow sections. The test results revealed that the failure modes of CFSST columns are generally similar to those of conventional carbon steel CFST columns. However, due to the increased ductility, the stainless steel composite columns showed far higher capacity of axial deformation and larger amplitudes of local outward bulges. The schematic failure modes of hollow steel tubes, CFST and CFSST are presented in Fig. 8.

Fig. 9 illustrates the typical measured axial load versus axial strain (N - ε) curves of the CFSST stub columns, where the axial load is normalised with respect to the maximum load N_{max}. Generally, the N- ε responses could be classified into three types, which depend mainly on the confinement of the stainless steel tube to concrete. If the confinement was strong enough, the N - ε relationship showed a strain-hardening response (Type A) with continuous strength increase from Point 1 to Point 2. As less confinement was provided, Type B curve had a strain-softening portion 1′2′ after reaching the first peak Point 1′. Because of the strong strain-hardening effect of stainless steel, the load increased once again to Point 3′ at the end of the test. Type C is the typical N–ε relationship with a strain-softening response which is very common for

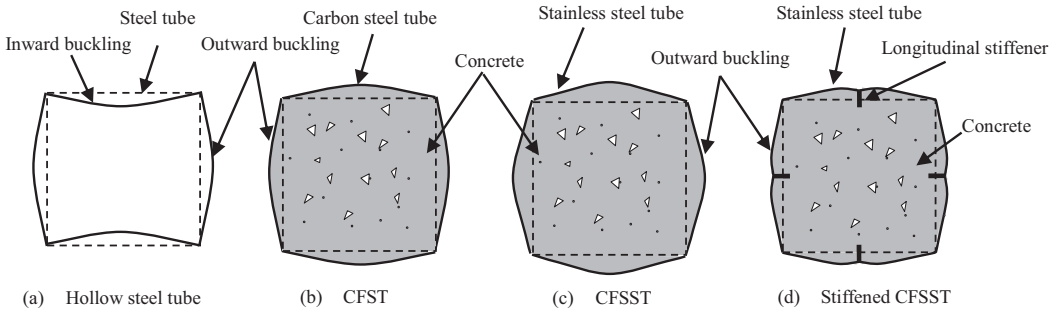

Fig. 8. Schematic failure modes of stub columns.

Please cite this article as: L.-H. Han, et al., Performance of concrete filled stainless steel tubular (CFSST) columns and joints: Summary of recent research, J Constr Steel Res (2017), https://doi.org/10.1016/j.jcsr.2018.02.038

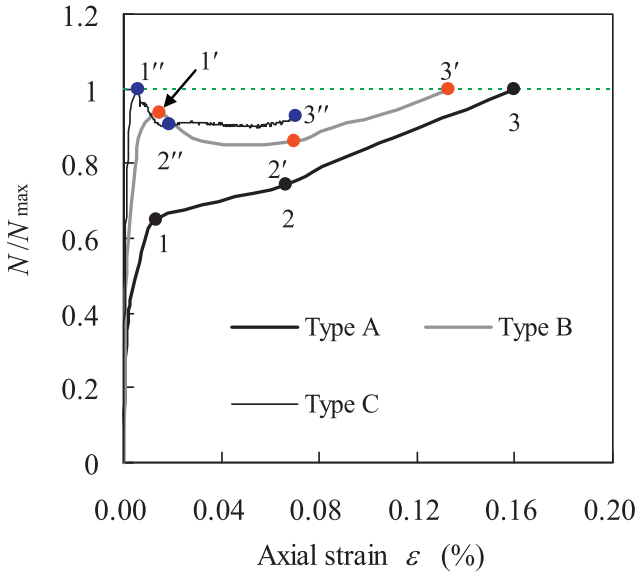

Fig. 9. Typical axial load (N) versus axial strain (ε) curves of CFSST stub columns.

conventional carbon steel CFST stub columns. Generally, the residual strength of the "Type C" CFSST stub column was much higher than that of a carbon steel composite counterpart. It is evident that the stainless steel tube could provide better confinement for its core concrete at the late loading stage compared with the carbon steel tube in a CFST column.

In order to examine the feasibility of using existing design codes to predict the ultimate strength of CFSST columns, the predictions from the Australian design code AS 5100 [55], American code ANSI/AISC 360-05 [56], Chinese code DBJ/T 13-51-2010 [57] and Eurocode 4 [58] were compared to the test results [4]. It was evident that all codes were conservative in predicting the load-carrying capacity of CFSST columns. For short columns under axial compression, AS 5100 gives the best predictions for circular columns, whilst DBJ/T offers the closest predictions for square columns. Meanwhile, all codes underestimate the capacity by 47–67% for short columns under compression and bending and about 11.1–25.5% for slender columns, respectively.

Compared with a carbon steel tube, the amplitudes of local buckles in the stainless steel tubes are much higher. According to the experiment reported in [4], the axial shortening of a CFSST can reach as high as 20% without the observation of possible fracture of the stainless steel tube due to the high ductility of stainless steel. To allow the use of thin-walled stainless steel tubes, Dabaon et al. investigated the effectiveness of welding longitudinal stiffeners in the inner face of a stainless steel tube by experiment [14] and finite element analysis [59]. The failure mode of the stiffened CFSST is illustrated in Fig. 8d. It can be concluded that the longitudinal stiffener can improve the strength of CFSST columns by postponing local buckling of the stiffened tube.

The above studies focused on CFSST columns with regular circular or square sections shown in Fig. 1. Han et al. [11] proposed another innovative type of composite members with a stainless steel jacket, i.e., stainless steel-concrete-carbon steel double-skin tubular (DST) columns, as shown in Fig. 10, where b and d are dimensions of the inner carbon steel tube; B and D are dimensions of the outer stainless steel tube; and t_{si} and t_{so} are the wall thicknesses of the inner and outer tubes, respectively. Compared with the conventional concrete filled double skin tubes, the use of the outer stainless steel tube will increase the corrosion resistance and aesthetics of the composite column. An experimental investigation was conducted on 80 specimens with different column types (straight, inclined and tapered) and cross-sectional types (circular, square, round-end rectangular and elliptical). The test results indicated that the stainless steel-concrete-carbon steel DST columns generally failed in a ductile manner with the outward local buckling of the outer stainless steel tubes and the inward buckling of the inner carbon steel tubes. It was evident that the inclined angle has a moderate influence on the load-carrying capacity of the inclined DST columns. However, the strength tended to decrease with the increase of the tapered angle for the tapered DST columns. A simplified model was also proposed in [11] for predicting the ultimate strength of stainless steel-concrete-carbon steel DST stub columns.

With the purpose of utilising the advantages of stainless steel at a reduced cost, Ye et al. [13] proposed an innovative concrete-filled bimetallic tube (CFBT) construction, where the cross section of the bimetallic tube is composed of an outer layer made of stainless steel and an inner layer made of carbon steel. A serial of experimental and numerical investigations were conducted in [13,60] on the behaviour of CFBT stub columns. It was found that the CFBT columns failed in a ductile manner, and the outer stainless steel tube layer could work well with the inner carbon steel tube layer during the whole loading process. The two layers of the bimetallic tube generally buckled at same positions at failure. A three-dimensional FE model was established to simulate circular CFBT stub columns subjected to axial compression [60]. A simplified model was then put forward to predict the ultimate strength of the circular CFBT stub columns.

Yang and Ma [7] and Chen et al. [17] reported test results on CFSST beams under pure bending. The results showed that both circular and rectangular CFSST beams fail in a very ductile manner. For the stainless tube, there was no tensile fracture in the tension zone, whilst local buckles appeared in the compression zone of beam at the mid-span. Meanwhile, crushing of concrete was observed at the locations where the stainless steel tube buckled. Similar to concrete-filled carbon steel tubes [61], the measured bending moment versus mid-span deflection curves for CFSST beams could be divided into three stages, i.e., initial elastic stage, inelastic stage and strain-hardening stage. The measured initial flexural

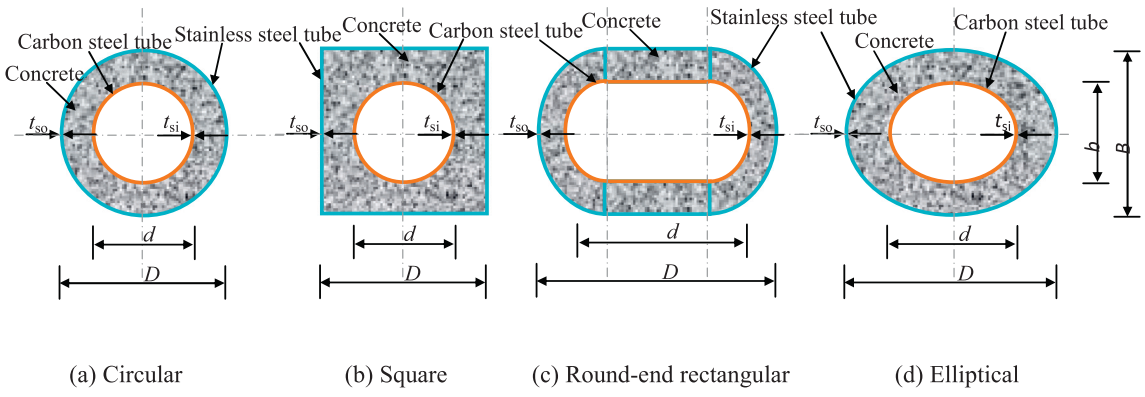

Fig. 10. Schematic view of stainless steel-concrete-carbon steel DST sections.

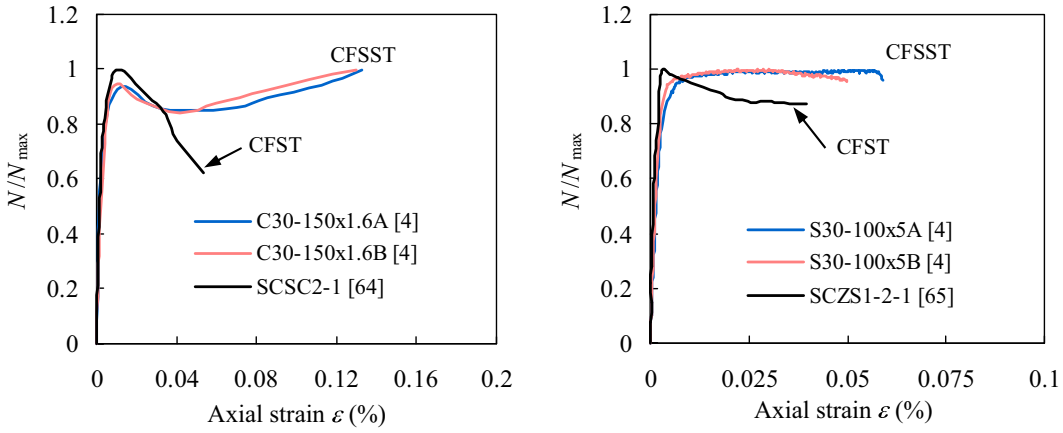

Fig. 11. Comparison of N- ε curves between CFSST and CFST stub columns.

stiffness and serviceability-level flexural stiffness of CFSST beams were compared with predictions from design codes of ANSI/AISC 360-05 [56], BS 5400-5 [62], DB21/T1746–2009 [63] and EC4 [58]. It was found that these codes give higher predictions compared with the test results. It seems that the material nonlinearity of stainless steel should be considered when determining the flexural stiffness.

A confinement factor (ξ) may be defined and used to describe the passive confinement of steel tubes on their concrete infill, i.e.,

$$\xi = \frac{A_s}{A_c} \cdot \frac{f_y}{f_{ck}} \tag{18}$$

where A_s and A_c are the cross-sectional areas of the steel and concrete, respectively; f_y is the yield stress of steel; and f_{ck} is the characteristic strength of the concrete.

To further evaluate the possible behaviour differences between stainless steel and carbon steel CFST columns, the N- ε curves of CFSST columns presented by Uy et al. [4] are compared with those carbon steel ones available in the literature [64,65]. For circular columns, the carbon steel specimen SCSC2-1 presented by Han and Yao [64] is compared with the CFSST specimens C30–150 × 1.6A and C30–150 × 1.6B [4]. All of them have a same ξ of 0.49. The carbon steel specimen SCZS1-2-1 with an ξ of 3.52 presented in [65] is compared with CFSST specimens S30-100x5A and S30-100x5B with an ξ of 3.59 [4]. Fig. 11 shows that the shape of the N- ε curve for a CFSST column is quite different from that of a carbon steel CFST column with a close confinement factor ξ. The CFSST column shows more gradual yielding behaviour owing to the fact that the nonlinear stress-strain curve of stainless steel is of the "roundhouse" type. More obviously, a CFSST column has much higher residual strength even after experienced large axial deformation compared with its carbon steel counterpart. This feature of CFSST columns makes them very favourable to be used as structural columns that are most likely to be subjected to extreme loads, like explosion, collision and fire exposure.

It was also found that the core concrete tends to exhibit more ductile behaviour as ξ increases in a CFSST column [18,66]. Fig. 12 shows a typical axial load (N/N_u) versus moment (M/M_u) interaction curve for CFSST short columns, where N_u and M_u are the axial compressive capacity and bending moment capacity, respectively. The shape of the interaction curve is similar to that of carbon steel CFST short columns. Further research is required to propose design equations to precisely represent the interaction curves.

5. Dynamic performance

Like conventional CFST columns, concrete filled stainless steel tubes also have good potential to be used in earthquake-prone zones. Liao et al. [18] carried out a series of tests on CFSST columns under constant axial load and cyclic lateral loading. The typical failure modes of circular and square specimens are illustrated in Fig. 13, including concrete crushing, and local buckling and/or fracture of the steel tube. The tested CFSST columns showed very plump lateral load versus lateral deflection (P–Δ) responses, indicating a high energy dissipation ability of the composite columns. Similar high levels of ductility and energy dissipation were observed in cyclic loading tests on concrete-filled double-skin (SHS outer and CHS inner) stainless steel tubular beam-columns carried out by Zhou and Xu [19]. Compared with conventional carbon steel CFST columns, the attained lateral displacements of CFSST columns are much higher whilst tensile fracture was less likely to occur after the application of the cyclic loading.

Fig. 14 compares the P–Δ hysteretic responses of CFSST and CFST columns, where the confinement factors (ξ) of them were selected to be close. Since the sizes of the columns were not exactly the same, the lateral load P and lateral deflection Δ were normalised with respect to the maximum load P_{max} and yield displacement Δ_y, respectively, to have a meaningful comparison. Both types of composite columns showed very plump hysteretic hoops without significant pinching effect. In general, the CFSST column displayed better energy dissipation ability under cyclic loading as compared with the CFST column. The axial load level was a crucial factor affecting the cyclic behaviour of composite columns. If a column was subjected to a large axial compressive load, it was the core concrete rather than the steel that determined the performance of the composite member. Thus, the difference between the CFST and

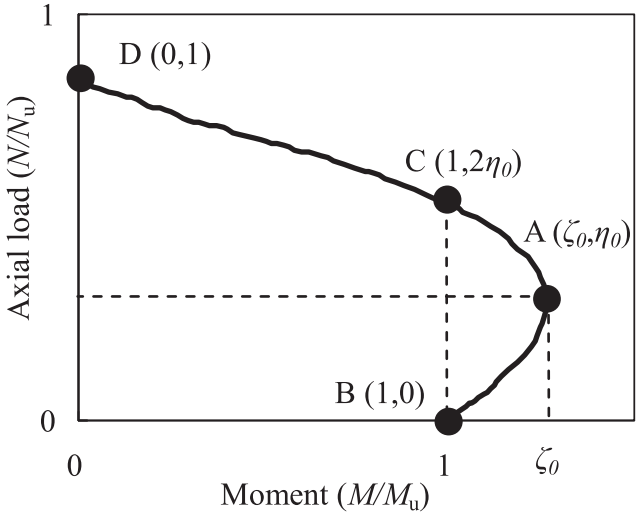

Fig. 12. Typical interaction curve of CFSST columns.

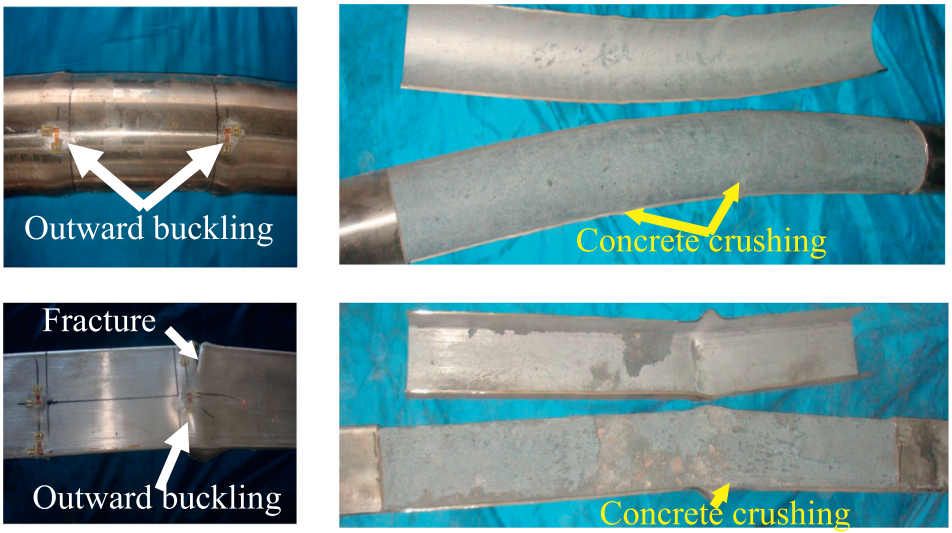

Fig. 13. Typical failure modes of circular and square CFSST subjected to cyclic lateral loading.

CFSST columns was generally negligible in terms of P–Δ hysteretic response when a high axial load level of 0.6 was applied, as shown in Fig. 14b. However, at a small axial load level ($n = 0.02$), the performance of a column was more significantly affected by the tensile behaviour of the steel. Therefore, the CFSST column with n of 0.02 exhibited more obvious hardening characteristic compared with the carbon steel counterpart, as shown in Fig. 14a. After reaching the peak load, the lateral load of the CFST column tended to decrease gradually, whereas that of the CFSST column still experienced significant hardening even under large lateral deformation. Moreover, a slight pinching effect was observed for the CFST column at a late loading stage, but that was not found for the CFSST column. This phenomenon is mainly attributed to the significant strain hardening effect of the stainless steel.

The American Specification ANSI/AISC 360-10 [67], Chinese code DBJ/T 13-51-2010 [57], and Eurocode 4 [58] were employed to predict the ultimate strength and flexural stiffness of the tested specimens [18]. It is evident that all the three codes underestimated the load-carrying capacities of CFSST columns under combined axial force and bending moment. The EC4 method gave the closest predictions for both circular and square CFSST columns. In predicting the flexural stiffness, the standard deviations are large for all design approaches because the dependency of the axial load is not accounted for. The AISC-360-10 and DBJ/T specifications optimistically predict the initial section flexural stiffness for $n = 0.02$, whereas the EC4 prediction is conservative. For higher axial load levels, the initial section flexural stiffness values are conservatively predicted by all the three specifications. For serviceability-level section flexural stiffness, the DBJ/T method gives the closest predictions for both the circular and square CFSST specimens.

CFSST columns subjected to transverse impact were experimentally and theoretically studied by Bambach [20] and Yousuf [21,22]. It was evident that the high ductility of stainless steel improves the energy absorption capability as CFSST columns can accommodate higher transverse deformation under transverse impact. Tests results from Yousuf [22] indicated that, the static and impact strengths of stainless steel hollow and CFSST columns were 30–46% higher than those of the mild steel hollow and CFST columns. FE models have been developed to predict the behaviour of CFSST members under transverse impact [22].

6. Fire performance

Fire performance of concrete filled stainless steel tubes is of interest to engineers concerned with the fire resistance of structures. Han et al. [23] conducted an experimental investigation on five full-scale CFSST columns in standard fire test conditions, where the length of the

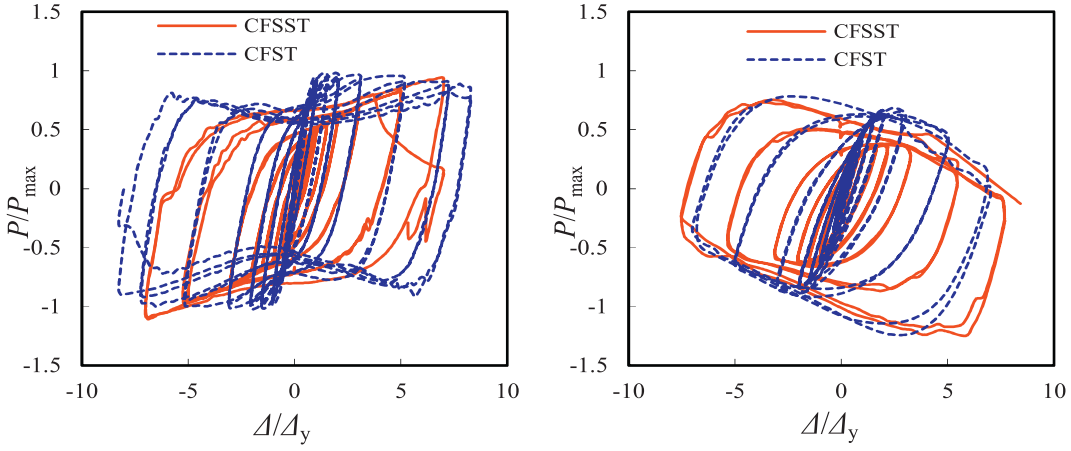

Fig. 14. Comparison of lateral load versus lateral deflection hysteretic curves between CFSST and CFST columns.

Please cite this article as: L.-H. Han, et al., Performance of concrete filled stainless steel tubular (CFSST) columns and joints: Summary of recent research, J Constr Steel Res (2017), https://doi.org/10.1016/j.jcsr.2018.02.038

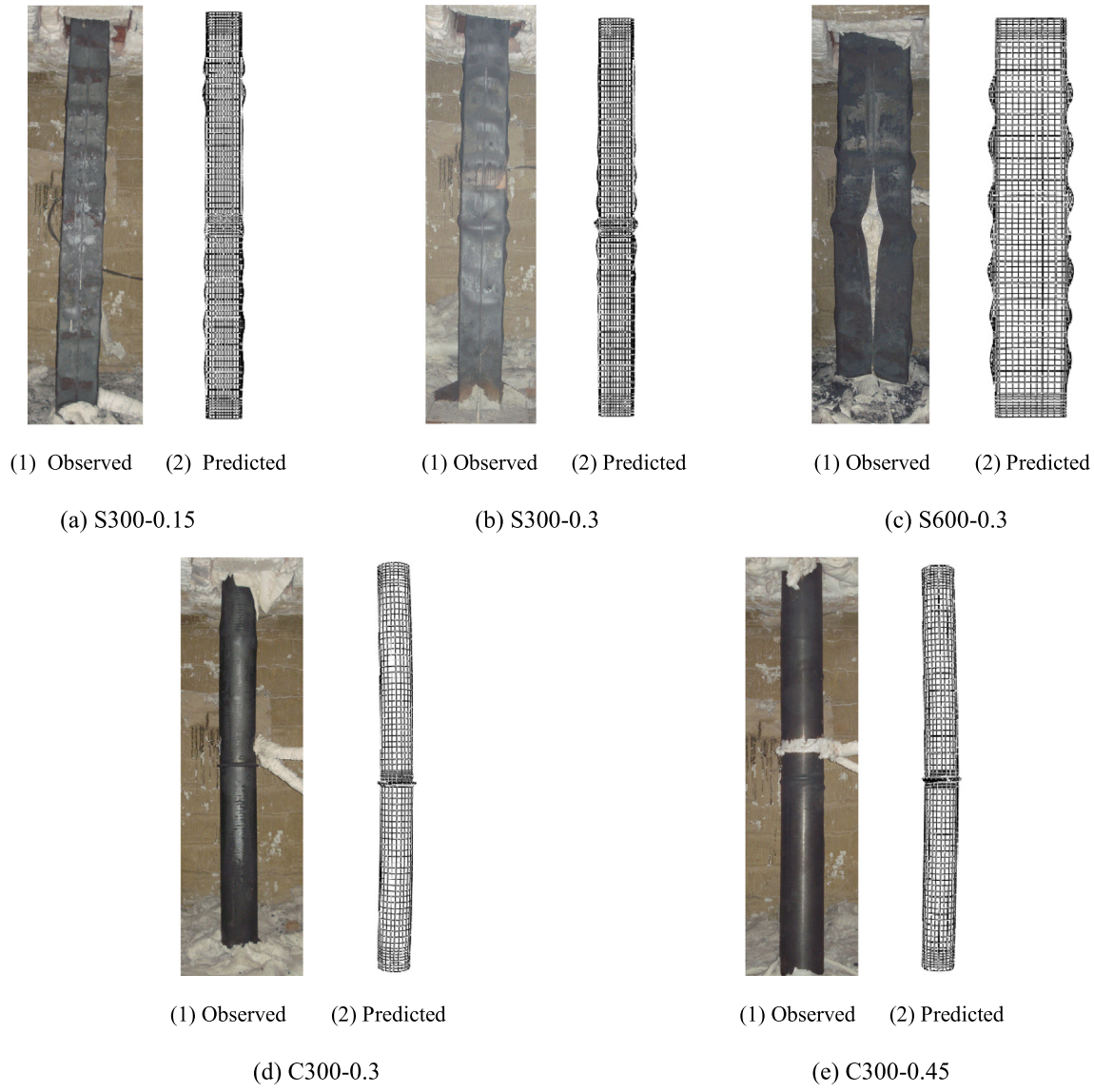

Fig. 15. Failure modes of specimens in full scale fire tests.

CFSST columns (L) was 3600 mm and the largest cross-sectional dimension was 630 mm. Grade S30408 (EN 1.4301 or AISI 304) austenitic stainless steel was used to manufacture the outer steel tubes which were infilled with self-consolidating concrete. The load level ($n_f = N_F/N_u$, where N_F is the applied axial compression load; and N_u is the load-bearing capacity of the column at ambient temperature) of the tested CFSST specimen ranged from 0.15 to 0.45. The tests were carried out in a column furnace in Tianjin Fire Research Institute, China. The temperatures in the furnace were controlled in accordance with ISO 834 standard fire curve. Fig. 15 presents the failure modes of the specimens after exposed to fire. For square CFSST specimens, local buckling appeared along the whole column length, where weld fracture of the stainless steel tube was observed at the place where severe local buckling occurred. For CFSST specimens with circular sections, local buckling of the steel tube was also observed, whereas the mode of buckling was different from that of the square section. Only one major elephant foot bulge was found at the mid-height of the column for the circular specimens. After removing the outer tube, it was evident that the core concrete and the stainless steel tube separated from each other at places where the local buckling had occurred.

A FE model was established in [23] to simulate the structural behaviour of CFSST columns in fire, and also to compare the fire performance between CFSST and CFST columns. It was clear that the fire resistance of the CFSST column is much higher than that of its CFST counterpart. In a typical calculating example, the fire resistance (R) increases from 48 to 82 min when stainless steel is used to replace carbon steel in a CFST column, mainly due to the superior material properties of stainless steel at elevated temperatures. A series of parametric studies were also performed by using the FE model, and two design tables (Tables 4 and 5) were then proposed to predict the fire resistance of CFSST columns,

Table 4
Design fire resistance (R) of circular CFSST columns (unit: min).

Slenderness ratio λ	Sectional dimension D (mm)	Load level n_F			
		0.3	0.4	0.5	0.6
20	300	110	70	45	25
	600	170	95	65	40
	900	230	130	85	50
40	300	80	55	35	25
	600	125	75	50	35
	900	150	90	60	45
60	300	65	45	30	20
	600	80	50	40	30
	900	100	60	50	40

Please cite this article as: L.-H. Han, et al., Performance of concrete filled stainless steel tubular (CFSST) columns and joints: Summary of recent research, J Constr Steel Res (2017), https://doi.org/10.1016/j.jcsr.2018.02.038

Table 5
Design fire resistance (R) of square CFSST columns (unit: min).

Slenderness ratio λ	Sectional dimension B (mm)	Load level n_F			
		0.3	0.4	0.5	0.6
17.3	300	110	70	45	25
	600	170	95	60	35
	900	220	120	75	45
34.6	300	95	65	45	25
	600	145	80	55	35
	900	160	95	65	45
52	300	75	50	35	20
	600	95	65	45	30
	900	125	85	60	40

where the slenderness ratio λ is determined as $4L/D$ for circular columns and $2\sqrt{3}L/B$ for square columns.

Tao et al. [24] also carried out tests on CFSST columns in fire and after fire exposure. The sectional size of the tested specimens was 200 mm and the load level ranged from 0.28 to 0.48. A total of 12 specimens were tested, including 6 CFSST columns in fire and another 6 post-fire CFSST columns. A three-dimensional FE model was also developed in [24] by introducing the measured initial imperfections and load eccentricities. It once again confirms that the fire resistance of carbon steel composite columns is much lower than that of their CFSST counterparts, as shown in Fig. 16, highlighting the benefits of using stainless steel. Meanwhile, it was found that the post-fire strength of circular CFSST specimens was not sensitive to fire exposure, whilst a strength loss up to 36% was observed for square specimens.

7. CFSST composite joints

If CFSST columns are to be applied in real buildings, reliable beam to column joints are crucial for transferring beams' loads to columns and ensuring structural safety. Tao et al. [25] carried out tests on seven full-scale joints with blind bolted connections to CFSST columns. As shown in Fig. 17, binding bars were used in three joint specimens with square columns to tie the opposite surfaces of the steel tube together. This aimed to increase the integrity of the panel zone. It was evident that the application of binding bars in the connection tended to increase the joint stiffness and strength, and reduce the separation between the steel tube and concrete. As shown in Fig. 18, by adding binding bars, the ultimate hogging moment capacity (M_{uh}) was improved by 10.7%, whilst the initial stiffness (K_{ih}) was improved by 62.5%. According

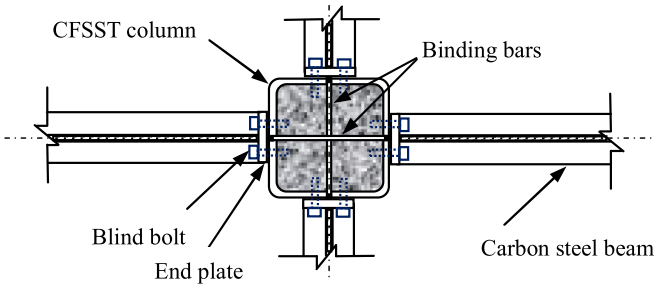

Fig. 17. Typical configuration of hybrid beam-column joints.

to Eurocode 3 [68], the blind bolted joint without composite slab could be classified as nominally pinned joint. However, in the presence of the floor slab, the joint nearly reached its full strength and the stiffness was also significantly increased close to the limit for rigid sway frames. In general, the adoption of stainless steel or carbon steel for the column had very minor influence on the joint behaviour.

Song et al. [28] conducted further fire tests on eight full-scale blind bolted joints with CFSST columns in the standard fire condition. The test results indicated that the blind bolted joint demonstrated very good performance in fire, and no bolt shank fracture or bolt pull-out failure was observed in the test. When the steel beam was protected, the fire resistance times of the blind bolted joints with CFSST columns ranged from 72 to 90 min. Meanwhile, it was found that the presence of the binding bars or the type of the steel tube (carbon or stainless steel) had only moderate influence on the fire resistance. It should be noted that the research conducted by Song et al. [28] only examined the fire performance of isolated blind bolted joints. Further experimental and theoretical studies should be conducted on beam-column assemblies with blind bolted connections to consider the influence of structural continuity and interaction. It will clarify if catenary action can develop in steel beams connected to columns by blind bolts.

Truss structures are widely used in engineering practice. Filling the chords with concrete can significantly improve the joint capacity and the fire resistance. Feng and Young [26,27] carried out a series of experiment to investigate the behaviour of concrete-filled high strength and normal strength stainless steel tubular T-joints and X-joints as shown in Fig. 19. It can be concluded that when there is a brace connected to the chord, local buckling failure of the brace is the main failure mode observed in both T and X joints specimens. For the joints with steel bearing plates, the measured limit-state loads were compared with the design strengths calculated using the current design rules for carbon steel

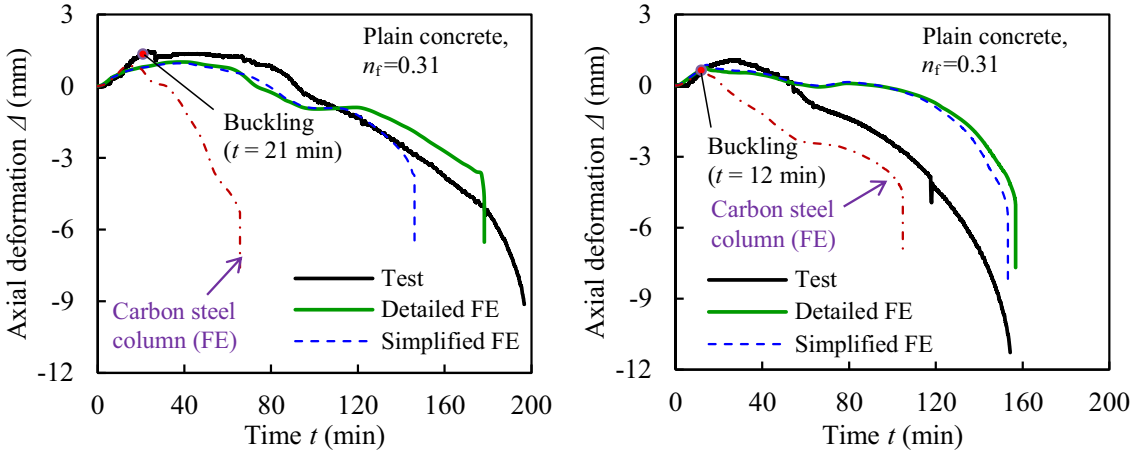

(a) Circular specimens (b) Square specimens

Fig. 16. Axial deformation (Δ) versus time (t) curves for fire-resistance test specimens.

Please cite this article as: L.-H. Han, et al., Performance of concrete filled stainless steel tubular (CFSST) columns and joints: Summary of recent research, J Constr Steel Res (2017), https://doi.org/10.1016/j.jcsr.2018.02.038

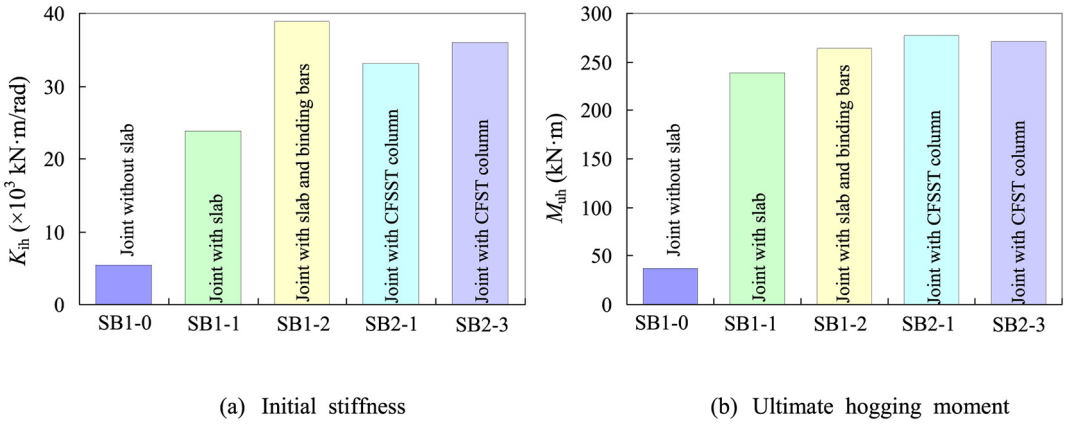

(a) Initial stiffness (b) Ultimate hogging moment

Fig. 18. Influence of testing parameters on K_{ih} and M_{uh} of joint specimens.

joints. It was found that the predicted strengths are generally conservative compared with the measured results. The significant contribution of stainless steel, which was not adequately considered in the current design rules for carbon steel joints, should be taken into account in the design rules for stainless steel T-joints and X-joints.

8. Concluding remarks

This paper reviewed some recent research on concrete filled stainless steel tubular (CFSST) structures. From the previous studies, it could be concluded that CFSST columns generally show improved ductility, higher energy dissipation ability, and superior fire performance compared with conventional CFST with carbon steel.

However, the bond strength should be emphasised in engineering practice. The bond strength between the stainless steel tube and core concrete in a CFSST column is 32–69% lower than that in a CFST column due to the smoother surface of the stainless steel. Although the bond strength is not a problem in normal service condition where the concrete and stainless steel tube are loaded simultaneously, this issue should be considered if a possible load transfer occurs between the steel tube and concrete via bond. If required, suitable measures can be taken to increase the bond strength, such as welding internal rings and shear studs, as well as using expansive concrete.

The existing codes for CFST columns with carbon steel, such as AS5100, AISC, DBJ/T and EC4, all underestimate the load-carry capacity of CFSST columns, mainly due to the fact that the strain hardening characteristic of stainless steel has not been beneficially considered. The feasibility of connecting CFSST columns to carbon steel beam by blind bolts has been examined, and the results showed that the composite joint exhibited favourable performance both at ambient temperature and in fire.

There are several possible future research directions. Firstly, more experiment research needs to be carried out to further study the mechanism of concrete filled stainless steel tubes, such as columns under tensile loading and torsion, and columns under long-term loading. Secondly, further theoretical research needs to be carried out for the purpose of development of more comprehensive design approaches for concrete filled stainless steel tubes. Thirdly, further research is needed to assist the structural fire design of CFSST columns. Performance-based approach is preferred since no heat insulation is expected to be provided for a CFSST column. Finally, more research attention should be paid to the joints and structures with CFSST columns.

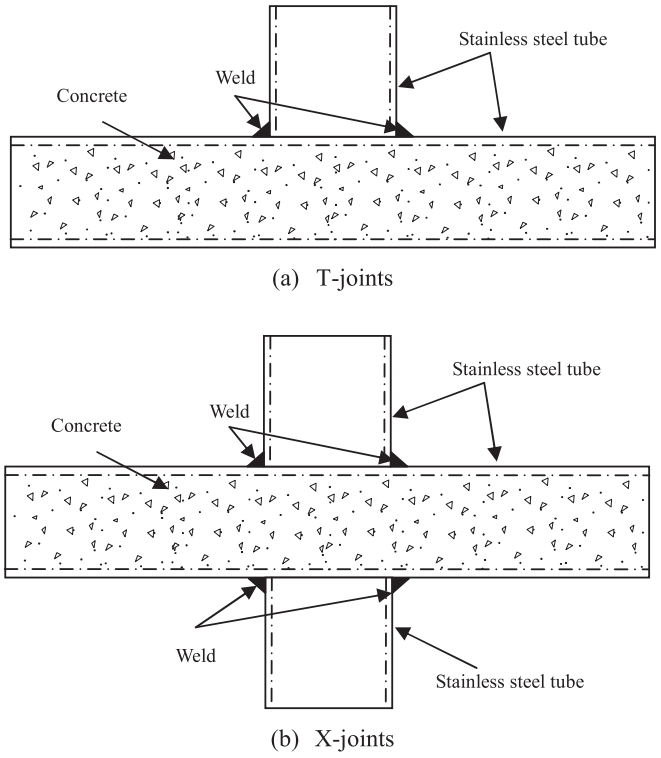

Fig. 19. Typical configurations of T-joints and X-joints.

References

[1] Z. Tao, T.Y. Song, B. Uy, L.H. Han, Bond behavior in concrete-filled steel tubes, J. Constr. Steel Res. 120 (2016) 81–93.
[2] Y. Chen, R. Feng, Y. Shao, X. Zhang, Bond-slip behaviour of concrete-filled stainless steel circular hollow section tubes, J. Constr. Steel Res. 130 (2017) 248–263.
[3] T.Y. Song, Z. Tao, L.H. Han, B. Uy, Bond behavior of concrete-filled steel tubes at elevated temperatures, J. Struct. Eng. ASCE 143 (11) (2017) 04017147.
[4] B. Uy, Z. Tao, L.H. Han, Behaviour of short and slender concrete-filled stainless steel tubular columns, J. Constr. Steel Res. 67 (3) (2011) 360–378.
[5] D. Lam, L. Gardner, Structural design of stainless steel concrete filled columns, J. Constr. Steel Res. 64 (11) (2008) 1275–1282.
[6] B. Young, E. Ellobody, Experimental investigation of concrete-filled cold-formed high strength stainless steel tube columns, J. Constr. Steel Res. 62 (5) (2006) 484–492.
[7] Y.F. Yang, G.L. Ma, Experimental behaviour of recycled aggregate concrete filled stainless steel tube stub columns and beams, Thin-Walled Struct. 66 (2013) 62–75.
[8] V.W.Y. Tam, Z.B. Wang, Z. Tao, Behaviour of recycled aggregate concrete filled stainless steel stub columns, Mater. Struct. 47 (1–2) (2014) 293–310.
[9] Y.L. Li, X.L. Zhao, R.K.R. Singh, S. Al-Saadi, Experimental study on seawater and sea sand concrete filled GFRP and stainless steel tubular stub columns, Thin-Walled Struct. 106 (2016) 390–406.
[10] Y.L. Li, X.L. Zhao, R.K.R. Singh, S. Al-Saadi, Tests on seawater and sea sand concrete-filled CFRP, BFRP and stainless steel tubular stub columns, Thin-Walled Struct. 108 (2016) 163–184.
[11] L.H. Han, Q.X. Ren, W. Li, Tests on stub stainless steel-concrete-carbon steel double-skin tubular (DST) columns, J. Constr. Steel Res. 67 (3) (2011) 437–452.
[12] F. Wang, B. Young, L. Gardner, Experimental investigation of concrete-filled double skin tubular stub columns with stainless steel outer tubes, Proceedings of the 8th International Conference on Steel and Aluminium Structures. Hong Kong, China, 2016.

Please cite this article as: L.-H. Han, et al., Performance of concrete filled stainless steel tubular (CFSST) columns and joints: Summary of recent research, J Constr Steel Res (2017), https://doi.org/10.1016/j.jcsr.2018.02.038

[13] Y. Ye, L.H. Han, T. Sheehan, Z.X. Guo, Concrete-filled bimetallic tubes under axial compression: experimental investigation, Thin-Walled Struct. 108 (2017) 321–332.
[14] M.A. Dabaon, M.H. El-Boghdadi, M.F. Hassanein, Experimental investigation on concrete-filled stainless steel stiffened tubular stub columns, Eng. Struct. 31 (2009) 300–307.
[15] E. Ellobody, M.F. Ghazy, Experimental investigation of eccentrically loaded fibre reinforced concrete-filled stainless steel tubular columns, J. Constr. Steel Res. 76 (2012) 167–176.
[16] S. Tokgoz, Tests on plain and steel fiber concrete-filled stainless steel tubular columns, J. Constr. Steel Res. 114 (2015) 129–135.
[17] Y. Chen, R. Feng, L. Wang, Flexural behaviour of concrete-filled stainless steel SHS and RHS tubes, Eng. Struct. 134 (2017) 159–171.
[18] F.Y. Liao, L.H. Han, Z. Tao, K.J.R. Rasmussen, Experimental behavior of concrete-filled stainless steel tubular columns under cyclic lateral loading, J. Struct. Eng. ASCE 143 (4) (2017) 04016219.
[19] F. Zhou, W. Xu, Cyclic loading tests on concrete-filled double-skin (SHS outer and CHS inner) stainless steel tubular beam-columns, Eng. Struct. 127 (2016) 304–318.
[20] M.R. Bambach, Design of hollow and concrete filled steel and stainless steel tubular columns for transverse impact loads, Thin-Walled Struct. 49 (10) (2011) 1251–1260.
[21] M. Yousuf, B. Uy, Z. Tao, A. Remennikov, J.R. Liew, Transverse impact resistance of hollow and concrete filled stainless steel columns, J. Constr. Steel Res. 82 (82) (2013) 177–189.
[22] M. Yousuf, B. Uy, Z. Tao, A. Remennikov, J.R. Liew, Impact behaviour of pre-compressed hollow and concrete filled mild and stainless steel columns, J. Constr. Steel Res. 96 (96) (2014) 54–68.
[23] L.H. Han, F. Chen, F.Y. Liao, Z. Tao, B. Uy, Fire performance of concrete filled stainless steel tubular columns, Eng. Struct. 56 (2013) 165–181.
[24] Z. Tao, M. Ghannam, T.Y. Song, L.H. Han, Experimental and numerical investigation of concrete-filled stainless steel columns exposed to fire, J. Constr. Steel Res. 118 (2016) 120–134.
[25] Z. Tao, M.K. Hassana, T.Y. Song, L.H. Han, Experimental study on blind bolted connections to concrete-filled stainless steel columns, J. Constr. Steel Res. 128 (2017) 825–838.
[26] R. Feng, B. Young, Tests of concrete-filled stainless steel tubular T-joints, J. Constr. Steel Res. 64 (11) (2008) 1283–1293.
[27] R. Feng, B. Young, Behaviour of concrete-filled stainless steel tubular X-joints subjected to compression, Thin-Walled Struct. 47 (4) (2009) 365–374.
[28] T.Y. Song, Z. Tao, A. Razzazzadeh, L.H. Han, K. Zhou, Fire performance of blind bolted composite beam to column joints, J. Constr. Steel Res. 132 (2017) 29–42.
[29] FABIG Technical Note 5, Design Guide for Stainless Steel Blast Walls, The Steel Construction Institute, Berkshire, UK, 1999.
[30] Eurocode 3, Design of Steel Structures Part1–4: General Rules-Supplementary Rules for Stainless Steel, British Standards Institution, London, UK, 2006.
[31] AS/NZS 4673, Cold-formed Stainless Steel Structures. Sydney, Standards Australia, Australia, 2001.
[32] BS EN 10088-1, List of Stainless Steels, British Standard Institution, British, 2014.
[33] ASTM A959, Standard Guide for Specifying Harmonized Standard Grade Compositions for Wrought Stainless Steels, Pennsylvania, USA, American Society for Testing and Materials, 2009.
[34] GB/T 20878-2007, Stainless and Heat-resisting Steel–Designation and Chemical Composition, Standard Press of China, Beijing, 2007 (in Chinese).
[35] BS EN 10088-2, Technical Delivery Conditions for Sheet/Plate and Strip of Corrosion Resisting Steels for General Purposes, British Standard Institution, British, 2014.
[36] Design Manual for Structural Stainless Steel. , The Steel Construction Institute, Berkshire, UK, 2017.
[37] K.J.R. Rasmussen, Full-range stress–strain curves for stainless steel alloys, J. Constr. Steel Res. 59 (1) (2003) 47–61.
[38] I. Arrayago, E. Real, L. Gardner, Description of stress–strain curves for stainless steel alloys, Mater. Des. 87 (2015) 540–552.
[39] Z. Tao, K.J.R. Rasmussen, Stress-strain model for ferritic stainless steels, J. Mater. Civ. Eng. 28 (2) (2016) 06015009.
[40] W.M. Quach, J.G. Teng, K.F. Chung, Three-stage full-range stress-strain model for stainless steels, J. Struct. Eng. 134 (9) (2008) 1518–1527.
[41] SEI/ASCE 8-02, Specification for the Design of Cold-formed Stainless Steel Structural Members, American Society of Civil Engineers, Reston, Virginia, USA, 2002.
[42] L. Gardner, D.A. Nethercot, Experiments on stainless steel hollow sections—part 1: material and cross-sectional behaviour, J. Constr. Steel Res. 60 (9) (2004) 1291–1318.
[43] X.Q. Wang, Z. Tao, T.Y. Song, L.H. Han, Stress–strain model of austenitic stainless steel after exposure to elevated temperatures, J. Constr. Steel Res. 99 (8) (2014) 129–139.
[44] R.B. Cruise, L. Gardner, Strength enhancements induced during cold forming of stainless steel sections, J. Constr. Steel Res. 64 (11) (2008) 1310–1316.
[45] M. Ashraf, L. Gardner, D.A. Nethercot, Finite element modeling of structural stainless steel cross-sections, Thin-Walled Struct. 44 (10) (2006) 1048–1062.
[46] L. Gardner, D.A. Nethercot, Numerical modeling of stainless steel structural components—a consistent approach, J. Struct. Eng. 130 (10) (2004) 1586–1601.
[47] E. Ellobody, B. Young, Structural performance of cold-formed high strength stainless steel columns, J. Constr. Steel Res. 61 (12) (2005) 1631–1649.
[48] M. Jandera, L. Gardner, J. Machacek, Residual stresses in cold-rolled stainless steel hollow sections, J. Constr. Steel Res. 64 (11) (2008) 1255–1263.
[49] Z. Tao, B. Uy, L.H. Han, Z.B. Wang, Analysis and design of concrete-filled stiffened thin-walled steel tubular columns under axial compression, Thin-Walled Struct. 47 (12) (2009) 1544–1556.
[50] B. Uy, Z. Tao, B.S. Chen, Dynamic behaviour of stainless steel investigated with a Split-Hopkinson tensile bar, International Conference on Shock and Impact Loads on Structures, 2009.
[51] Eurocode 3, Design of Steel Structures Part 1-2: General Rules-Structural Fire Design, British Standards Institution, London, UK, 2005.
[52] L. Gardner, K.T. Ng, Temperature development in structural stainless steel sections exposed to fire, Fire Saf. J. 41 (3) (2006) 185–203.
[53] K.T. Ng, L. Gardner, Buckling of stainless steel columns and beams in fire. Steel, Construction 29 (5) (2008) 717–730.
[54] Z. Tao, X.Q. Wang, M.K. Hassan, T.Y. Song, Mechanical behaviour of three types of stainless steel after exposure to elevated temperatures, Stainless Steel in Structures: Fifth International Experts Seminar, The Steel Construction Institute, London, UK, 2017.
[55] Standards Australia, Bridge Design, Part 6: Steel and Composite Construction. AS 5100.6-2004. Sydney (Australia), 2004.
[56] ANSI/AISC 360-05, Specification for Structural Steel Buildings, American Institute of Steel Construction, Chicago (IL, USA), 2005.
[57] DBJ/T 13-51-2010, Technical specification for concrete-filled steel tubular structures, The Department of Housing and Urban–Rural Development of Fujian Province, Fuzhou (China), 2010 (in Chinese).
[58] Eurocode 4, Design of Composite Steel and Concrete Structures Part 1-1: General Rules and Rules for Building, CEN, Brussels, 2004.
[59] M.A. Dabaon, S. El-Khoriby, M.H. El-Boghdadi, M.F. Hassanein, Confinement effect of stiffened and unstiffened concrete-filled stainless steel tubular stub columns, J. Constr. Steel Res. 65 (8) (2009) 1846–1854.
[60] Y. Ye, L.H. Han, Z.X. Guo, Concrete-filled bimetallic tubes (CFBT) under axial compression: analytical behaviour, Thin-Walled Struct. 119 (2017) 839–850.
[61] L.H. Han, Flexural behaviour of concrete-filled steel tubes, J. Constr. Steel Res. 60 (2) (2004) 313–337.
[62] BS 5400-5, Steel, concrete and composite bridges, Part 5: Code of Practice for the Design of Composite Bridges, British Standards Institution, 2005.
[63] DB21/T1746-2009, Technical Specification for Concrete-filled Steel Tubular Structures. Liaoning, China, 2009 (in Chinese).
[64] L.H. Han, G.H. Yao, Experimental behaviour of thin-walled hollow structural steel (HSS) columns filled with self-consolidating concrete (SCC), Thin-Walled Struct. 42 (9) (2004) 1357–1377.
[65] L.H. Han, X.L. Zhao, Z. Tao, Tests and mechanics model for concrete-filled SHS stub columns, columns and beam-columns, Steel Compos. Struct. 1 (1) (2001) 51–74.
[66] Z. Tao, B. Uy, F.Y. Liao, L.H. Han, Nonlinear analysis of concrete-filled square stainless steel stub columns under axial compression, J. Constr. Steel Res. 67 (11) (2011) 1719–1732.
[67] ANSI/AISC 360-10, Specification for Structural Steel Buildings, American Institute of Steel Construction, Chicago (IL, USA), 2010.
[68] Eurocode 3, Design of Steel Structures - Part 1-8: Design of Joints. EN 1993-1-8: 2005(Brussels, Belgium) 2005.

Please cite this article as: L.-H. Han, et al., Performance of concrete filled stainless steel tubular (CFSST) columns and joints: Summary of recent research, J Constr Steel Res (2017), https://doi.org/10.1016/j.jcsr.2018.02.038